# IMPROVED MAPPING SOLUTION USING TERRESTRIAL LASER SCANNERS AND LOW-COST UAV IMAGES

## Akram AFIFI, Ahmed EL-RABBANY, Canada

**Key words**: Unmanned Aerial Vehicle (UAV), Laser Scanner, Point cloud

## SUMMARY

This paper provides an improved mapping solution through the fusion of terrestrial laser scanner point cloud data and low-cost unmanned aerial vehicles (UAV) images. The terrestrial laser scanner (TLS) data are collected with the FARO Focus S scanner in different setups and resolutions, while the UAV images are captured with low-cost DJI phantom 4 pro UAV. A number of ground control points and targets, whose precise coordinates are determined using virtual reference stations (VRS) GPS, are used to enhance the image acquisition and registration. In addition, a number of targets are established throughout the scanned structure, which are precisely positioned using both of GPS and traditional surveying techniques. Such targets are used to enhance the accuracy of point cloud registration. Photoscan (Agisoft Inc.) and Autodesk ReCap Pro software packages are used to verify the image registration, along with MATLAB and CloudCompare software. Both of the laser scanner's point cloud and the UAV images are used to create a 3D model of the scanned structure and surroundings. It is shown that combining different sensor data enables detailed information about the area and objects of interest. In addition, a multi-sensor data fusion produced a complete 3D mapping solution, which has no gaps or missing objects.

# IMPROVED MAPPING SOLUTION USING TERRESTRIAL LASER SCANNERS AND LOW-COST UAV IMAGES

**Akram AFIFI, Ahmed EL-RABBANY, Canada**

## 1. Abstract

This paper provides an improved mapping solution through the fusion of terrestrial laser scanner point cloud data and low-cost unmanned aerial vehicles (UAV) images. The terrestrial laser scanner (TLS) data are collected with the FARO Focus S scanner in different setups and resolutions, while the UAV images are captured with low-cost DJI phantom 4 pro UAV. A number of ground control points and targets, whose precise coordinates are determined using virtual reference stations (VRS) GPS, are used to enhance the image acquisition and registration. In addition, a number of targets are established throughout the scanned structure, which are precisely positioned using both of GPS and traditional surveying techniques. Such targets are used to enhance the accuracy of point cloud registration. Photoscan (Agisoft Inc.) and Autodesk ReCap Pro software packages are used to verify the image registration, along with MATLAB and CloudCompare software. Both of the laser scanner's point cloud and the UAV images are used to create a 3D model of the scanned structure and surroundings. It is shown that combining different sensor data enables detailed information about the area and objects of interest. In addition, multi-sensor data fusion produced a complete 3D mapping solution, which has no gaps or missing objects.

## 2. INTRODUCTON

Typically, low-cost small unmanned aerial vehicles (UAV) carry low resolution imaging system, which may not be suitable for topographic surveying. To enhance the mapping accuracy of such a system, it is essential that a well-distributed ground control points (GCP) are established. FARO Focus S terrestrial laser scanner (TLS) is used as the main scanning system to capture point cloud data from different locations in the area of interest. Unfortunately, however, the area covered by TLS is limited and the quality of the 3D data depends on the scanning angles. Therefore, in this study, a UAV carrying a RGB camera with a field of view of 84° and a focal length of 8.8 mm, is used to obtain an additional coverage of the mapped area in a short time (Hopkinson et al., 2004, Van der Zande et al., 2006).

Two data sets are collected by FARO Focus S TLS and a low-cost camera installed on board the DJI Phantom 4 Pro UAV, respectively. A number of ground control points, whose precise coordinates are determined using SOKKIA GCX2 receiver in the VRS mode, are used to enhance the image acquisition and registration, which are used to improve the accuracy of the point cloud registration. In addition, a number of targets are created and placed at specific locations throughout the scanned structure. The precise coordinates of these targets are precisely determined using GPS and traditional surveying techniques. Agisoft Photoscan and Autodesk ReCap Pro software packages are used to verify the registration process, along with MATLAB and CloudCompare. Both of the laser scanner's point cloud and the UAV images are used to create a 3D model of the scanned structure and surroundings.

Figure 1. FARO Focus S TLS and Phantom 4 pro UAV (DJI, 2018; Faro Inc, 2018)

In this paper, raw data sets acquired by UAV and TLS are combined to obtain detailed information about the objects of interest. The structured point cloud captured by the TLS and unstructured point cloud that are created from the UAV camera images are used to generate separate 3D models. The TLS 3D point cloud have several gaps, glass features, and no rooftop. The UAV-generated 3D point cloud, on the other hand, doesn't include object under canopies. The data fusion allowed for the production of a complete 3D mapping solution with no gaps or missing features.

## 3. EXPERIMENTS

Low-cost DJI Phantom 4 Pro UAV is used in this study, which is equipped with a 20-megapixel camera and a single-frequency GPS receiver. Unfortunately, the UAV positioning solution is based on a consumer-grade low-cost GPS receiver, which limits the positioning precision to meter level. Figure 2 shows the estimated UAV camera position for a total of 342 images and their corresponding error ellipses.
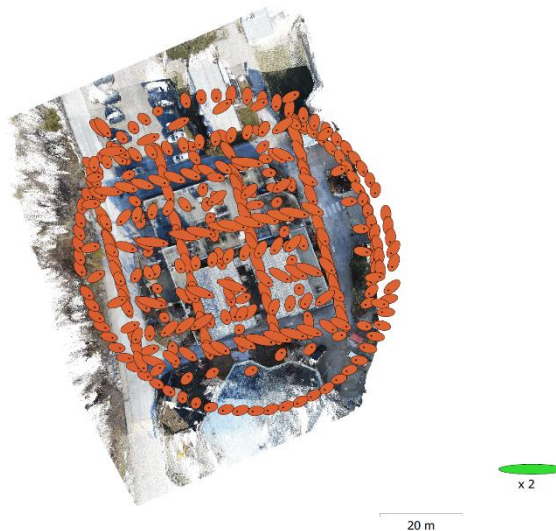


Figure 2 UAV camera position and the corresponding error ellipse.
Uncertainties in the East and North components are represented by error ellipses. Estimated camera locations are marked with a black dot.

As shown in Figure 2, the consumer-grade UAV GPS produces a positioning solution, which includes a large error due to its limited capability. Table 1 shows the estimated total error in the overall 3D mapping output using the UAV GPS coordinates.

Table 1. shows the estimated error in the East and North UAV location

| East Error (m) | North Error (m) | Total Error (m) |
|---|---|---|
| 0.913 | 1.122 | 1.408 |

GCPs were used to calibrate the UAV camera using an adaptive camera model fitting as shown in Table 2. The adaptive camera model enables automatic selection of the camera parameters to be included in the adjustment process based on their reliability estimates (Agisoft, 2018). Data sets with strong camera geometries, such as images taken for all sides of a building, help fix more parameters during initial camera alignment. The intrinsic specifications are scale factors for each axis, coordinates of the origin of image planes and the intersection of the optical axis with the image plane. The Euclidean transformation that yields the camera image frames 3-dimensional position and orientation in space with respect to the fixed world frame represents the extrinsic characteristics of the camera system and is independent of the cameras intrinsic parameters (Pomares et al., 2007).

Table 2. Calibration coefficients and correlation matrix

|  | Value | Error | F | Cx | Cy | K1 | K2 | K3 | P1 | P2 |
|---|---|---|---|---|---|---|---|---|---|---|
| B1 | -0.37718 |  |  |  |  |  |  |  |  |  |
| B2 | 0.347872 |  |  |  |  |  |  |  |  |  |
| K4 | -0.06506 |  |  |  |  |  |  |  |  |  |
| F | 3652.76 | 0.059 | 1 | -0.06 | -0.81 | -0.12 | 0.19 | -0.17 | -0.04 | -0.45 |
| Cx | -25.4714 | 0.032 |  | 1 | 0.06 | 0 | 0 | -0.01 | 0.9 | 0.03 |
| Cy | 4.97314 | 0.047 |  |  | 1 | -0.11 | 0 | 0.01 | 0.04 | 0.73 |
| K1 | 0.008973 | 3.90E-05 |  |  |  | 1 | -0.96 | 0.9 | 0 | -0.16 |
| K2 | -0.05879 | 0.00011 |  |  |  |  | 1 | -0.98 | 0 | 0.04 |
| K3 | 0.108221 | 0.0001 |  |  |  |  |  | 1 | -0.01 | -0.04 |
| P1 | -0.00129 | 3.10E-06 |  |  |  |  |  |  | 1 | 0.03 |
| P2 | 0.000252 | 3.20E-06 |  |  |  |  |  |  |  | 1 |

Where, F is the focal length measured in units of pixels; cx, cy are the coordinates of the principal point; b1, b2 are affinity and skew (non-orthogonality) transformation coefficients; k1, k2, k3, k4 are radial distortion coefficients; p1, p2, p3, p4 are tangential distortion coefficients.

The sequential photos captured by the UAV camera are used for 3D construction of the objects through the Photoscan software, as shown in Figure 3. The 3D objects created by the UAV camera images are georeferenced through the onboard GPS in the World Geodetic System 1984 (WGS84) reference frame (DJI, 2018).

Figure 3. 3D model created using SfM software, Photoscan (Agisoft, 2018)

To improve the 3D mapping accuracy, the XYZ coordinates of the 3D data created by the UAV-SfM and TLS are georeferenced using a number of GCPs and on-structure targets. A total of eight GCPs are established within the UAV mission location. The layout and distribution of the GCPs are designed to satisfy a good coverage for different flight scenarios, including the image strips, and ability to obtain a good satellite geometry when occupying each of them. A total of 16 object targets are designed and fixed to the building walls at different heights as shown in Figure 4.
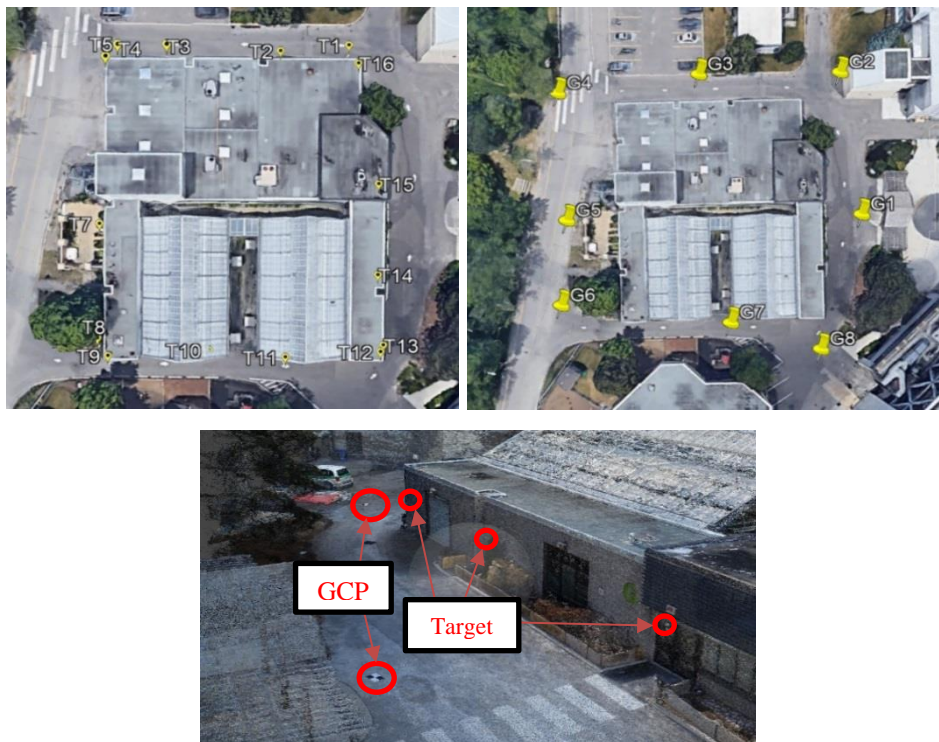


Figure 4 GCPs and structure targets

The GCPs are designed to be visible from the UAV camera. As such the size a GCP was selected to be 43.18 cm by 55.88 cm as shown in Figure 5. The object targets are distributed throughout the structure to ensure visibility from both of the TLS and UAV. Therefore, the object targets were designed to be 21.59 cm by 13.97 cm as shown in Figure 5. Unfortunately, during the field data acquisition target T6 was lost and therefore all data related to it is ignored in the processing.
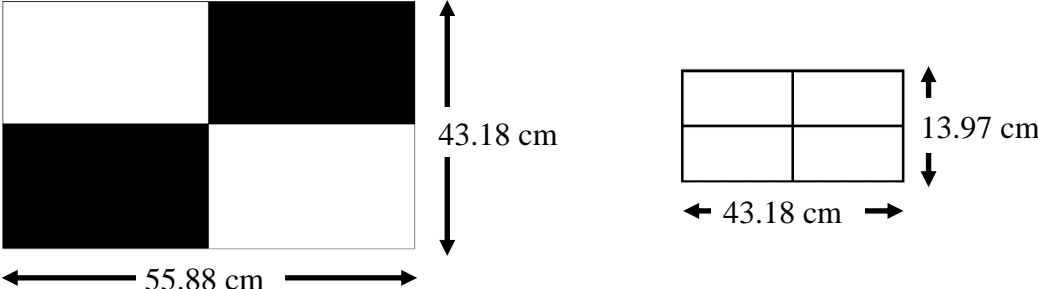


Figure 5 GCP and object target

The GCP coordinates were obtained using a dual-frequency GPS receiver in the VRS mode. The object targets are captured using a total station with a GCP back-sighted. Table 3 shows the GCP positioning error in the 3D model.

Table 3. Ground control points positioning error

| Label | Positioning Error (cm) | | | Total (cm) |
|---|---|---|---|---|
| | East | North | Altitude | |
| G1 | -0.8 | -0.8 | 3.3 | 3.5 |
| G2 | 3.1 | 2.1 | -6.0 | 7.0 |
| G3 | -1.7 | -2.0 | 3.2 | 4.1 |
| G4 | -0.4 | -1.8 | 3.6 | 4.0 |
| G5 | 2.9 | -2.1 | 1.6 | 3.9 |
| G6 | 1.9 | -0.1 | -2.6 | 3.2 |
| G7 | 2.8 | 1.7 | 1.4 | 3.6 |
| G8 | 0.4 | 1.7 | -2.9 | 3.4 |
| Total | 2.0 | 1.7 | 3.3 | 4.3 |

To verify the accuracy of the data fusion technique, the object targets that are visible in the UAV images are used as check points. Table 4 shows the object targets position errors.

Table 4. Object targets positioning errors results from the 3D model

| Point | Positioning Error (cm) | | | Total (cm) |
|---|---|---|---|---|
| | East | North | Altitude | |
| T1 | 4.4 | 2.8 | -4.8 | 7.1 |
| T2 | -1.6 | -1.7 | 2.5 | 3.5 |
| T3 | -1.6 | -1.9 | 3.5 | 4.3 |
| T4 | -0.6 | -0.7 | 2.2 | 2.4 |
| T5 | -0.1 | -1.0 | 1.7 | 2.0 |
| T7 | 0.4 | -1.6 | -4.4 | 4.7 |

| | | | | |
|---|---|---|---|---|
| T8 | 0.4 | 0.0 | -2.5 | 2.5 |
| T11 | 0.5 | 0.9 | -1.5 | 1.8 |
| T12 | 0.1 | 1.5 | -2.8 | 3.2 |
| T13 | -3.4 | 0.2 | 5.1 | 6.1 |
| T14 | -2.5 | -0.4 | 4.2 | 4.8 |
| T16 | 4.3 | 2.0 | -5.2 | 7.0 |
| Total | 2.3 | 1.5 | 3.6 | 4.5 |

Figure 6 shows the GCP and check point positioning errors and their corresponding error ellipses.
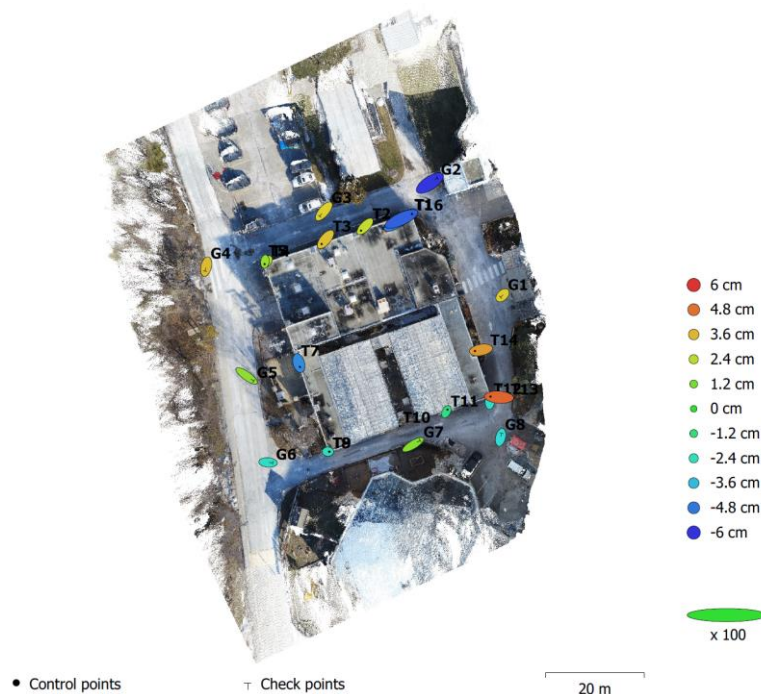


Figure 6 GCP and check points position errors and corresponding error error ellipses. Altitude error is represented by the color of the error ellipse. East, North errors are represented by the size of the error ellipse. Estimated GCP locations are marked with a dot and the check points with a cross.

A total of 28 setups were needed to capture the 360-degree scans with a 0.6mm point cloud precision at a 10 m distance from the scanner. Table 5 shows the TLS sensor specifications that has been used in this study.

Table 5. TLS sensor specifications

| Sensor name | Wavelength (nm) | Maximum distance | Vertical range (Deg) | Field of View (Deg) | Speed points/second |
|---|---|---|---|---|---|
| FARO Focus 3D S150 | 905 | 153.5 | 270 | 360 | 976,000 |

The FARO Focus 3D has a built-in GPS receiver. However, the GPS signal reception was rather poor because of the presence of tree canopy and/or building obstruction. As such, the accuracy

of the resulting scanner coordinates were rather poor and could not be used to register the 3D point cloud. Likewise, although the signal reception at the GPS receiver attached to the UAV was good, the precision of the obtained coordinates was around 10 m. As a result, there was a shift between the georeferenced TLS and UAV data.

The TLS data, which were acquired from different locations around the building, were processed and different point clouds were created and registered together through object targets system. A single 3D point cloud was produced from all the scans. The TLS was setup at 28 points around the structure to capture all the details and to create a good overlap between the scans as shown in Figure 7.
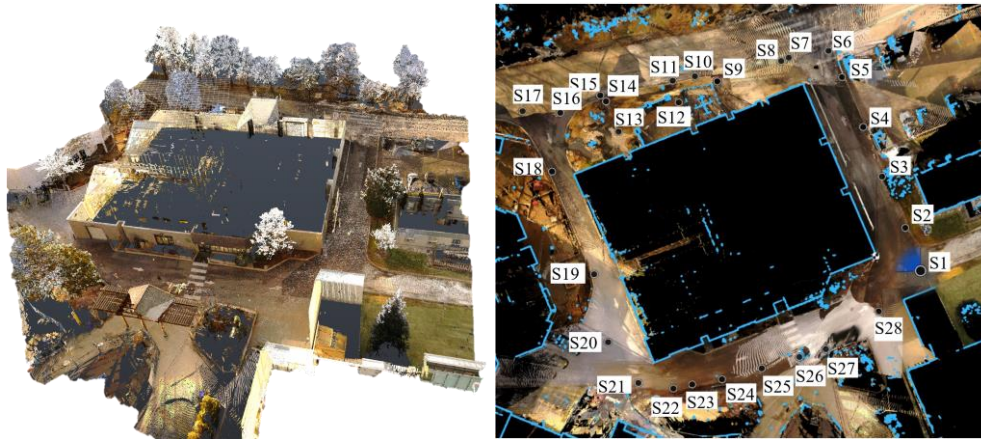


Figure 7. TLS scan locations and 3D model

## 4. RESULTS AND DISCUSSION

The point cloud generated from the UAV images are known as unstructured point cloud because they are generated based on features, location, and intensity. However, the TLS point cloud are generated based on the TLS mechanical rotation as shown in Figure 8.



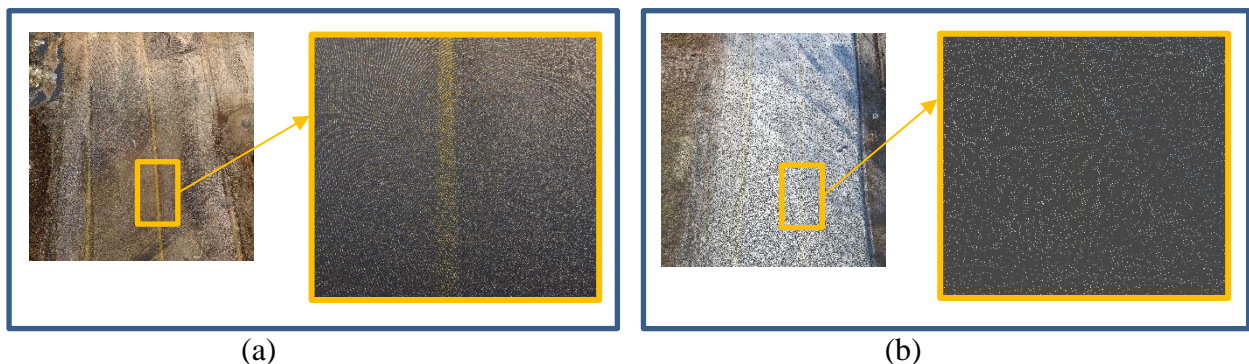(a)                                              (b)

Figure 8. TLS, structured point cloud (a) and UAV, unstructured point cloud (b)

The UAV and TLS data sets have different characteristics. While the TLS produces more structured and dense point cloud with some gaps, the UAV images provides a complete 3D data set, including glass surfaces. The results of UAV and TLS data fusion show a denser point cloud with no gaps, including the rooftop of the building. The data fusion output shows approximately a 5 cm positioning error. Figure 9 shows the 3D model results from the UAV and TLS data fusion.

Figure. 9 3D model of UAV and TLS data fusion

## 5. SUMMARY

In this paper, the fusion workflow of UAV and TLS point clouds is presented, which aims to obtain detailed information about the objects of interest. A number of GCP and object targets, whose coordinates are precisely determined by GPS in the VRS mode, are used to improve the 3D modeling accuracy for both of the UAV and TLS data. An adaptive camera model is used to calibrate the UAV camera, which takes advantage of the precise coordinates of ground control points. The structured TLS-based 3D point cloud have several gaps, glass features, and no rooftop. The unstructured UAV-based 3D point cloud, on the other hand, miss objects under canopies. It has been shown that fusing the two point clouds overcomes the limitations of both sensor data acquisitions and enables a complete 3D mapping solution, which includes detailed information about the area and objects of interest.

**REFERENCES**

Agisoft, 2018. Agisoft PhotoScan User Manual: Professional Edition, Version 1.4 Publication date 2018. Available at: http://www.agisoft.com/pdf/photoscan-pro_1_4_en.pdf

Pomares, J., Chaumette, F., and Torres, F., 2007. Adaptive Visual Servoing by Simultaneous Camera Calibration. Proceedings 2007 IEEE International Conference on Robotics and Automation, Roma, 2007, pp. 2811-2816. doi: 10.1109/ROBOT.2007.363897

DJI, 2018, phantom 4 pro specifications, available at: https://www.dji.com/phantom-4-pro/info

Faro Inc, 2018, FARO Focus3D performance specifications, available at: http://www.gb-geodezie.cz/wp-content/uploads/2016/01/FARO_-Focus_3D.pdf

Hopkinson, C., Chasmer, L., Young-Pow, C., Treitz, P., 2004. Assessing forest metrics with a ground-based scanning lidar., Canadian Journal of Forest Research 34(3), 573-583.

Van der Zande, D., Hoet, W., Jonckheere, I., van Aardt, J., Coppin, P., 2006. Influence of measurement set-up of ground-based LiDAR for derivation of tree structure, Agriculture and Forest Meteorology 141(2), 147-160

## BIOGRAPHICAL NOTES

**Akram Afifi** obtained his PhD degree in Geomatics Engineering from the Department of Civil Engineering, Ryerson University, Canada. He is currently a professor in the School of Applied Technology, Humber Institute of Technology and Advanced Learning. He also holds an adjunct professor position in the Department of Civil Engineering, Ryerson University. Akram's areas of expertise include Satellite Navigation, Smart Mapping Solutions, Land Surveying, Geographic Information Systems, Unmanned Aviation Systems, Laser/LiDAR Scanning and Geodesy. Akram received numerous awards in recognition of his academic and leadership achievements, including the Dennis Mock award from Ryerson University.

**Ahmed El-Rabbany** obtained his PhD degree in GPS Satellite Navigation from the Department of Geodesy and Geomatics Engineering, University of New Brunswick, Canada. At present, Dr. El-Rabbany is a full professor at Ryerson University, where he leads research projects in the areas of satellite navigation and multi-sensor integration.

## CONTACTS
Dr. Akram Afifi
Humber Institute of Technology and Advanced Learning
205 Humber College Blvd
Toronto
Canada
Tel. +1-416-675-6622 ext. 5434
Email: akram.afifi@humber.ca
Web site: https://appliedtechnology.humber.ca/